Antiferromagnetism in $CaCu_3Ti_4O_{12}$ studied by magnetic Raman spectroscopy

A. Koitzsch,[1] G. Blumberg,[1,*] A. Gozar,[1] B. Dennis,[1] A. P. Ramirez,[1,2] S. Trebst,[1] and Shuichi Wakimoto[3,†]

[1]*Bell Laboratories, Lucent Technologies, Murray Hill, New Jersey 07974*
[2]*Los Alamos National Laboratory, Los Alamos, New Mexico 87545*
[3]*Brookhaven National Laboratory, Upton, New York 11973*
and Massachusetts Institute of Technology, Cambridge, Massachusetts 02139

For $CaCu_3Ti_4O_{12}$—an insulator that exhibits a giant dielectric response above 100 K—Cu^{2+} antiferromagnetic spin ordering has been investigated by magnetic Raman scattering and magnetization measurements. Below the Néel temperature, $T_N = 25$ K, magnetic excitations have been identified. Above T_N Raman spectra reveal short-range antiferromagnetic fluctuations that increase with cooling like T^{-1}. No deviations from Curie-Weiss law have been observed above T_N.

Recently the insulating cubic compound $CaCu_3Ti_4O_{12}$ has attracted much interest because of its giant change in the dielectric response with temperature. This compound possesses a low-frequency dielectric constant, $\epsilon \sim 10^4$, which is only weakly varying in the temperature range 100–600 K. Below 100 K however, there is an abrupt 100-fold reduction in the value of ϵ but no structural phase transition that is usually associated with a large dielectric response has been observed. X-ray diffraction and thermodynamic data argue against an explanation in terms of collective ordering of local dipole moments.[1,2] It has been suggested that at low temperatures a redistribution of electric charge in the unit cell occurs accompanied by strong changes in the relaxational characteristic of dipolar fluctuations.[3] The $CaCu_3Ti_4O_{12}$ magnetic structure has been investigated by neutron diffraction and susceptibility measurements.[4,5] The system is antiferromagnetic below the Néel temperature $T_N = 25$ K.

In this paper, we investigate the magnetic properties of $CaCu_3Ti_4O_{12}$ single crystals by Raman spectroscopy, magnetization, and heat-capacity measurements. The data reveal local antiferromagnetic fluctuations between room temperature and T_N that rapidly strengthen with cooling like T^{-1}. This surprising result cannot be explained by frustration effects since the magnetization exhibits no deviations from the Curie-Weiss law and the Weiss constant is very close to the T_N value.

Figure 1 shows the crystal structure of $CaCu_3Ti_4O_{12}$, a cubic perovskitelike compound with space group $Im3$ (point group T_h).[6] Important features of this structure are the TiO_6 octahedrons, which are considered to be responsible for the giant electrical polarizability. If the position of the Ti^{4+} ion slightly shifts with respect to the oxygen cage local dipole moments arise. Because of the tilted arrangement of the octahedrons the ordering of the dipole moments is frustrated and no ferroelectric phase transition has been observed.[1,2] However, the Ti-O bonds are set under tension.

Figure 2 shows the heat-capacity and magnetization measurements that indicate an antiferromagnetic phase transition at 25 K with a Weiss constant of $\theta_W = -30$ K. $1/\chi$ is linear with temperature showing Curie-Weiss behavior almost to T_N. The Cu^{2+} ions carry a hole with spin $S = 1/2$ in the $3d$ shell, giving rise to magnetic moments that order antiferro-

magnetically due to the superexchange interaction. According to the Goodenough rules[7] it has been suggested[8] that the superexchange between the copper spins is promoted via the titanium ions rather than via the usual oxygen path. However, the interactions are expected to be weak.

The arrangement of the Cu^{2+} spins and thus the magnetic structure is shown in Fig. 3. We consider the effective exchange integrals J_1, J_2, and J_3 between nearest, next-nearest and third-nearest neighbors. The spins are ordered antiferromagnetically along the (111) direction with a ferromagnetic alignment in the [111] planes.[5]

Several excitations of the magnetic ground state by photon-induced spin exchange are possible. Direct one-magnon excitations, which correspond to the reversal of a single spin by spin-orbit or magnetic dipole-dipole interaction, are weak and can be identified by splitting in a magnetic field.[9] In most cases the spectra are dominated by two-magnon excitations that correspond to exchanging the positions of two neighboring spins. The underlying mechanism is the following: the incoming photon ω_i creates a virtual electron-hole state consisting of an excitation across the
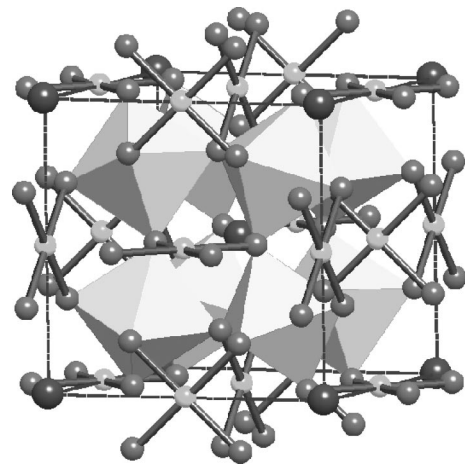

FIG. 1. Crystal structure of $CaCu_3Ti_4O_{12}$. The unit cell is built up by the atoms inside the dotted lines. It contains eight distorted TiO_6 octahedrons, copper atoms bonded to four oxygen atoms, and large Ca atoms at the edges and in the middle without drawn bonds.
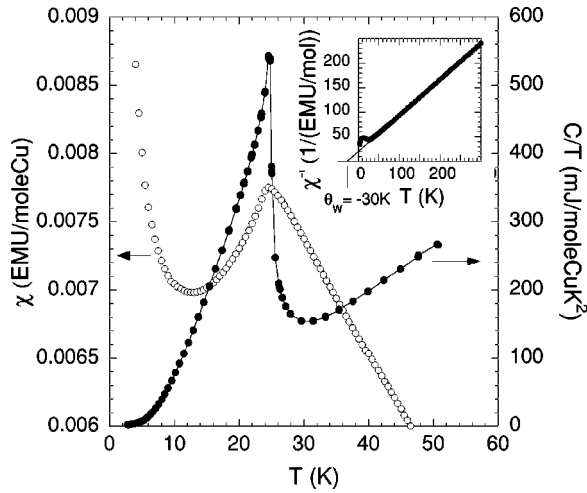
FIG. 2. Magnetization and heat-capacity measurements of $CaCu_3Ti_4O_{12}$. Shown are χ and C/T vs temperature. The antiferromagnetic phase transition occurs at $T_N = 25$ K. The inset shows the inverse susceptibility $1/\chi$ vs T with a Weiss constant of $\theta_W = -30$ K.

optical gap; then the fermions emit two magnons at energies ω_M (one by each fermion) with momenta q and $-q$ before recombining by emitting an outgoing photon with the energy loss $\omega_j = \omega_i - 2\omega_M$. The energy loss is the result of the perturbed spin position with respect to the ground state.[10] Possible two-magnon excitations would correspond to the exchange of the spin in position 1 with the spins in position $1'$ or $2'$. As will be shown below these processes can be resolved spectroscopically. Furthermore the magnetic behavior above T_N can be investigated and compared to the magnetization measurements.

Single crystals of $CaCu_3Ti_4O_{12}$ were grown by the

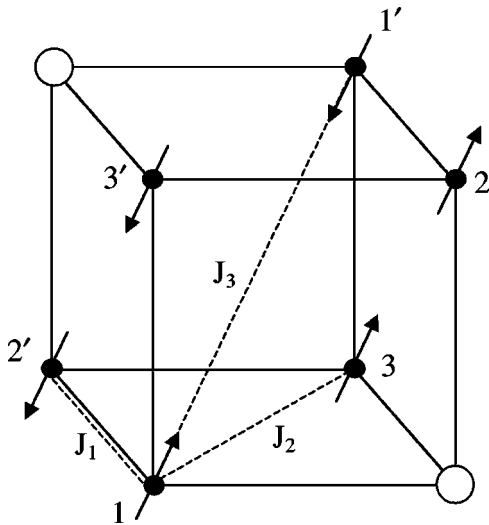FIG. 3. Spin structure of $CaCu_3Ti_4O_{12}$. The copper (black) and calcium (white) atoms of the lower right front eighth of the unit cell (Fig. 1) are shown. The TiO_6 octahedron is neglected for clarity. Each Cu^{2+} ion carries a spin, pointing in the (111) or ($\bar{1}\bar{1}\bar{1}$) direction. J_1, J_2, and J_3 are the exchange integrals between nearest, next-nearest and third-nearest neighbors.

traveling-solvent floating-zone method using a four-ellipsoidal mirror type image furnace. Dried starting materials of $CaCO_3$, CuO, and TiO_3 were mixed and baked at 800 °C and 850 °C for 24 h each with intermediate grindings to make the single-phase powder of $CaCu_2Ti_3O_{12}$. The feed rod was formed by a rubber tube in a hydrostatic press, and baked in air at 900 °C for 12 h. The pelletized solvent with the composition of $CaCu_2Ti_3O_4 : TiO_2 = 80 : 20$ in molar ratio was placed between the feed rod attached to the upper shaft and a seed attached to the lower shaft and was melted at the focal point. Each growth was performed for ~ 8 h with the growth speed of 6 mm/h in an oxygen atmosphere. During the growth, the upper and lower shafts rotated at 30 rpm in opposite directions of each other to mix the molten zone. The typical crystal size was 5 mm in diameter and 20 mm in length.

Raman measurements were performed from the [100] surface of the crystal mounted in a continuous helium flow optical cryostat. All spectra were taken in a backscattering geometry with excitations from a Kr^+ laser. The laser power was less than 10 mW and was focused to a 50 μm diameter spot on the sample surface. The spectra were analyzed by a custom triple grating spectrometer. All spectra were corrected for the spectral response of the spectrometer and detector. The temperatures were corrected for laser heating.

In Fig. 4, we present the temperature dependence of the Raman response of $CaCu_3Ti_4O_{12}$ in parallel $[z(xx)z]$ and cross $[z(xy)z]$ polarizations for blue excitation with $\omega_i = 2.6$ eV. The intense peaks at high frequency are identified as phonons. From the polarization dependence shown in Fig. 4 and spectra taken for $[z(x+y, x+y)z]$ and $[z(x+y, x-y)z]$ polarizations after sample rotation by 45°, we conclude that the 500 cm^{-1} phonon in cross polarization has T_g symmetry, the phonons at 450 and 520 cm^{-1} in parallel polarization obey A_g symmetry and the phonon at 580 and 300 cm^{-1} have E_g symmetry.

With cooling a new feature develops at low frequencies for the $[z(xy)z]$ polarization with a broad peak forming above T_N and a sharp structured band below T_N, suggesting a magnetic origin for these excitations. To exclude a possible one magnon origin, we applied an 8 T magnetic field. No shift or splitting of the peak was observed in the field confirming its singlet two-magnon nature. In parallel polarization the peak is strongly suppressed. Its polarization dependence reveals T_g symmetry, typical for two-magnon excitations. The inset in Fig. 4(b) shows the low frequency part of the spectra with red excitation $\omega_i = 1.65$ eV for which the two-magnon intensity is suppressed. This demonstrates the resonance behavior of the two-magnon excitation. The magnon intensity is expected to be sensitive to the excitation energy because the photon-induced spin-exchange process involves a virtual electron-hole excitation to a higher energy level.[10] If the excitation energy is close to interband transitions a resonance enhancement occurs.

Figure 5 shows the low-frequency region of the Raman response. The spectral shape depends strongly on the temperature. Four temperature regions are distinguishable. Above 70 K the spectra are basically flat and show weak features. Only small deviations from the background are vis-
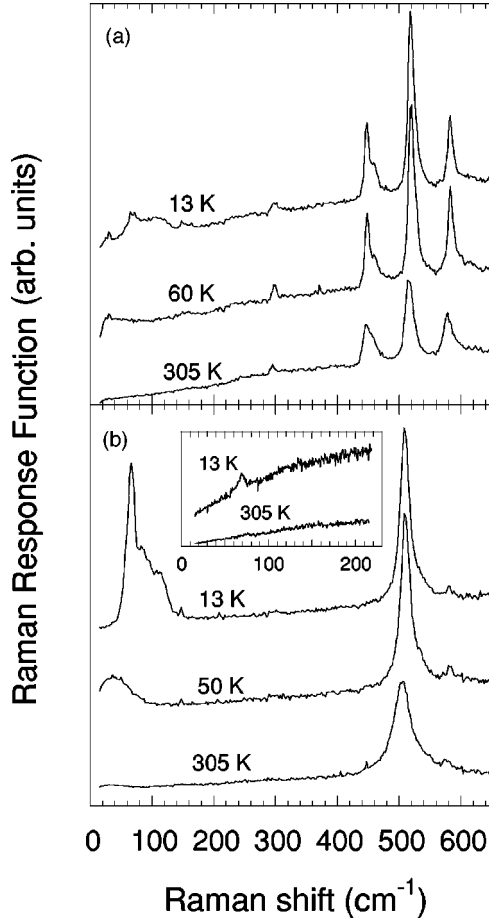
FIG. 4. Raman spectra in parallel (a) and cross (b) polarization for different temperatures using an excitation laser wavelength of $\lambda = 482.5$ nm. The peaks at 450, 520, and 580 cm^{-1} in the parallel polarization and 500 cm^{-1} in cross polarization correspond to phonons. The low-frequency band in cross polarization corresponds to two-magnon excitations. The inset shows spectra for excitation with $\lambda = 752$ nm in cross polarization. The magnon intensity is suppressed indicating resonant behavior.

ible. Below 70 K a clear peak develops around 35 cm^{-1}. The peak has a rather broad shape and its intensity grows with decreasing temperature. At 25 K, the value of the antiferromagnetic phase transition, the peak shifts to higher energies and the shape becomes more structured. Below 25 K a sharp structured two-magnon band with three components A, B, and C at 66, 87, and 112 cm^{-1} is observed. The two-magnon excitation has been fitted with three Lorentzians between 50 and 130 cm^{-1} (solid line). The left inset shows the intensity development of the magnetic excitation above and below T_N with a linear background intensity subtracted. The intensity increases monotonically with decreasing temperature and the antiferromagnetic phase transition does not immediately alter the slope. The fit shows that the intensity of the fluctuations (above T_N) is proportional to T^{-1}. Note that the intensity enhancement occurs in the temperature region of the anomalous T dependence of the dielectric constant. The peak positions in the right inset are constant above the Néel temperature and increase suddenly around 30 K. A slight anomaly is observed around 100 K.
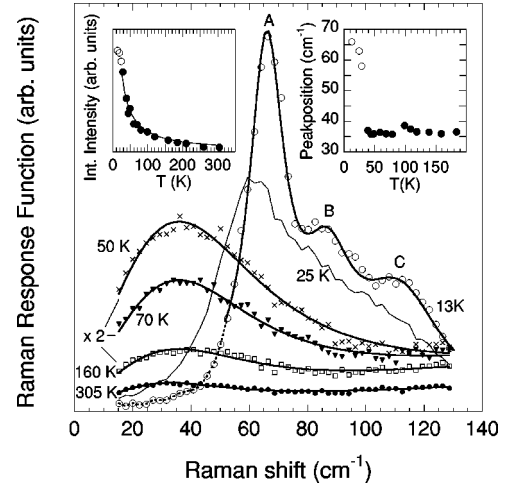

FIG. 5. Low-frequency excitations of $CaCu_3Ti_4O_{12}$ in cross polarization. Below T_N the excitation consists of a clear peak (A) at 66 cm^{-1} and two shoulders (B and C) at 87 and 112 cm^{-1}. The spectra above T_N are fitted with a damped harmonic oscillator function and are enlarged by a factor of 2 for comparison with the magnon peak. The 13 K spectra is fitted with three Lorentzians. The left inset shows the integrated intensity of the magnetic excitations above T_N (filled circles) and below T_N (empty circles) fitted with $I(T) \sim T^{-1}$. The right inset shows the peak positions of the excitations above T_N and peak A below T_N.

We explain the three components of the two-magnon band below 25 K with the different spin-exchange processes described above. We suggest that the two excitations at 66 and 87 cm^{-1} arise from the spin exchanges in positions 1 and 2' (along J_1) and 1 and 1' (along J_3). The exchange along J_2 gives no effect. Thus the highest excitation at 112 cm^{-1} could be a four-magnon process with instantaneous exchanges of two neighboring spin pairs. To estimate J_i ($i = 1,2,3$), we calculated the spin-exchange energies by counting the interaction energies given by

$$H = \sum_{\langle k,l \rangle} J_i^{kl} (\mathbf{S}_k \cdot \mathbf{S}_l), \tag{1}$$

where $\mathbf{S}_k$ and $\mathbf{S}_l$ are the vectors of neighboring spins and the sum is over nearest-neighbor, next-nearest-neighbor, and third-nearest-neighbor sites ($i = 1,2,3$ correspondingly). The energy of the two-magnon components correspond to the difference between the total magnetic energy calculated by Eq. (1) before and after the spin exchange. Thus, we yield a set of three linear equations to combine with three excitation energies. The highest energy must correspond to the assumed four-magnon process, reducing the number of solutions to two. One solution gives ferromagnetic exchange (and is, therefore, unphysical) the second gives antiferromagnetic exchange with $J_1 = 23$, $J_2 = 3$, and $J_3 = 2$ cm^{-1}. According to this solution, we assign feature A in Fig. 5 to the $1 \leftrightarrow 2'$ spin exchange, feature B to $1 \leftrightarrow 1'$ and feature C to $1 \leftrightarrow 2'$ and $2 \leftrightarrow 1'$ (a double spin exchange). Note that the double spin exchange $1 \leftrightarrow 2'$ and $2 \leftrightarrow 3'$ yields similar results. The Weiss constant is approximately given by $k_B \theta_W = -J_1 + 2J_2 - 2J_3$, thus $\theta_W = -31$ K is in good agreement with the ex-

periment. Our value of $J_1 = 23 \, \text{cm}^{-1}$ is somewhat smaller than $J_1 = 34 \, \text{cm}^{-1}$ estimated in Ref. 5 and we obtain $J_1 \gg J_2, J_3$ instead of $J_3 \gg J_1, J_2$ as predicted in Ref. 8. However our minimal model has no adjustable parameters and the result is consistent with the magnetization measurements.

Above the Néel temperature no magnon excitation is expected. We ascribe the peak around $35 \, \text{cm}^{-1}$ to local antiferromagnetic spin fluctuations, e.g., to excitations of locally ordered spins, which we identify as overdamped magnons. Above T_N the long-range magnetic order is thermally destroyed. Nevertheless, on a short-range scale spin fluctuations persist and can be excited by light. The fluctuations reduce the number of spins that respond to an external field and contribute to the susceptibility. Since the intensity of the overdamped magnons measured by Raman increases with cooling a deviation from linearity of the inverse susceptibility is expected. In spite of that the susceptibility is in agreement with the Curie-Weiss law almost down to T_N as can be seen in Fig. 2. Therefore, we conclude that the fluctuations are emphasized by the resonant Raman response.

The microscopic origin of the T^{-1} dependence of the intensity of the fluctuations is not obvious. We suggest that the proposed charge redistribution in the unit cell at low temperatures that increases the ionicity of the bonds may enhance the superexchange interaction and hence the intensity of the fluctuations. On the other hand when the temperature is increased the giant dielectric response is observed and the intensity of the fluctuations drops. Assuming that the increase in ϵ is due to a displacement of the Ti^{4+} inside the TiO_6 octahedra, one expects the fluctuations be disturbed if Ti^{4+} is essential for the superexchange interaction as is proposed by Ref. 8. In this sense the increase of ϵ with temperature is accompanied by a decrease of the fluctuations.

In conclusion, we have investigated the low-frequency magnetic excitations of $CaCu_3Ti_4O_{12}$ using Raman spectroscopy. Below the Néel temperature $T_N = 25 \, \text{K}$ magnetic excitations are identified as a three component two-magnon band. The exchange integrals are estimated within the framework of the Heisenberg interaction model. Short-range magnetic fluctuations well above T_N were observed to develop with cooling as T^{-1}. A possible connection between dielectric and magnetic behavior is discussed.

---

*Corresponding author. Email address: girsh@bell-labs.com

†Present address: Department of Physics, University of Toronto, Toronto, Ontario M5S 1A7, Canada.

[1] M. A. Subramanian, Dong Li, N. Duan, B. A. Reisner, and A. W. Sleight, J. Solid State Chem. **151**, 323 (2000).

[2] A. P. Ramirez, M. A. Subramanian, M. Gardel, G. Blumberg, D. Li, T. Vogt, and S. M. Shapiro, Solid State Commun. **115**, 217 (2000).

[3] C. C. Homes, T. Vogt, S. M. Shapiro, S. Wakimoto, and A. P. Ramirez, Science **293**, 673 (2001).

[4] A. Collomb, D. Samaras, B. Bochu, and J. C. Joubert, Phys. Status Solidi A **41**, 459 (1977).

[5] Y. J. Kim, S. Wakimoto, and S. M. Shapiro (unpublished).

[6] B. Bochu, M. N. Deschizeaux, J. C. Joubert, A. Collomb, J. Chenavas, and M. Marezio, J. Solid State Chem. **29**, 291 (1979).

[7] J. B. Goodenough, *Magnetism and the Chemical Bond* (Interscience, New York, 1963)

[8] C. Lacroix, J. Phys. C **13**, 5125 (1980).

[9] P. A. Fleury and R. Loudon, Phys. Rev. **166**, 514 (1968).

[10] B. S. Shastry and B. I. Shraiman, Phys. Rev. Lett. **65**, 1068 (1990); A. V. Chubukov and D. M. Frenkel, *ibid.* **74**, 3057 (1995).